

Correlation of Viscoelastic Behavior with Model Thermal Testing

R. B. KRUSE* AND W. R. MAHAFFEY†
Thiokol Chemical Corporation, Huntsville, Ala.

A model test vehicle is discussed which is a cylindrically perforated right circular cylinder with an L/D ratio of 6, bonded without liner to a steel case. Diameters of the internal perforations have been varied from 0.200 to 1.000 in., permitting a variety of strains at any given temperature. Upon cooling a motor to successively lower temperature (temperature equilibrium is assumed), a temperature is reached at which failure occurs; when motors of several different core sizes are tested concurrently, it is, therefore, possible to define a failure threshold in terms of strain and temperature. Failure has been observed at temperatures ranging from -85° to $+50^\circ\text{F}$. Experimental data are presented which show that failure cannot be predicted from simple tensile tests in the 1-min^{-1} strain rate range, presumably due to rate effects. Strain endurance, another approach to failure prediction, is also shown to be rate-dependent; in this case, the strain endurance capability is found to be a function of the rate at which the strain was imposed.

Discussion

ALTHOUGH many of the tests discussed in this paper were designed with the specific goal of duplicating prototype motor conditions, sufficient data of a fundamental nature were obtained to permit certain conclusions to be drawn, at least tentatively, regarding inherent propellant response to biaxial stresses imposed by thermal conditioning. The present discussion concerns the relationship of mechanical properties as measured in the laboratory to motor structural performance under isothermal or transient temperature conditions.

If simple grain geometries are involved, the isothermal problem is fairly straightforward, even though a general time-dependent failure criterion has not been established. Furthermore, many currently used composite solid propellants seem to possess reasonably linear viscoelastic behavior until catastrophic failure of the specimen is imminent. It is, therefore, possible to use classical viscoelastic stress analysis as an approach to most isothermal problems.

On the other hand, when temperature is permitted to vary, particularly under transient temperature conditions, the problem of prediction of propellant grain failure becomes complex from the analytical standpoint because the governing equations become nonlinear. Because of this complexity, several solid-propellant development facilities have resorted to model testing for propellant evaluation. A properly designed model test vehicle acts as a link between laboratory measurements of propellant mechanical properties and operational performance of a prototype solid rocket motor.

To examine more adequately the problems of structural integrity and solid propellant mechanics inherent in a case-bonded solid propellant rocket motor, suitable model test vehicles have been developed to investigate the performance of propellant in a motor geometry.^{1, 2} The test vehicle developed by Thiokol consists of a 2-in.-i.d. steel tube 12-in. long, containing propellant with cavity diameters ranging from 0.200 to 1.000 in. Since the core sizes used in the test vehicles are generally too small to allow direct measurement of the cavity diameter with a profile recorder, as was done on larger motors, radiographic techniques have been employed

to measure the internal profile of the test motor in each preselected thermal or environmental condition.

With very small internal perforations, the test vehicle seems to be too short to produce the stresses or strains near the half-length position expected from infinite length analysis. Analysis can be made, however, by using the finite-length numerical solutions obtained by Parr.³ Alternatively, a longer specimen could be used. It is important to recognize, however, that, regardless of the port ratio, the L/D ratio of the motor, or of the Poisson's ratio of the material, the stresses or strains to be expected along the internal perforation can be considered known analytically, providing one is prepared to make the conventional assumptions of isotropy, homogeneity, and small strains. Thus, the tangential strain, equal to the diametral extension divided by the original perforation diameter, is used as a theoretical and experimental measure of the strain capability of the motor, varying as the temperature is changed. Assuming the thermal coefficient of expansion of the motor case to be negligible compared to that of the propellant, the case to be much more rigid than the propellant, and the propellant to be incompressible, one arrives at the Lamé solution for the tangential strain at the internal surface of the test vehicle during a steady-state temperature change⁴:

$$\epsilon_\theta = \left[-\frac{b^2}{a^2} + 1 \right] \frac{3\alpha T}{2} \Big|_{T_1}^{T_2} \quad (1)$$

where

$$b^2/a^2 = \lambda^2 \quad 3\alpha \equiv \beta$$

and where b is the outer diameter of the motor and a the inner diameter of the motor, so that

$$\epsilon_\theta = [(\lambda^2 - 1)/2]\beta\Delta T \quad (2)$$

The foregoing assumptions may be relaxed only at the expense of a considerable increase in algebraic complexity. The elastic solution is assumed to be valid under the near-equilibrium conditions involved, and the tangential strain, therefore, becomes a function of the volumetric coefficient of thermal expansion β and a grain geometry factor expressed in terms of the ratio of the outer diameter to the inner diameter of the propellant. The effect of cure shrinkage, usually considered as a constant, may also be included in Eq. (2) to yield

$$\epsilon_\theta = [(\lambda^2 - 1)/2]\beta\Delta T + \Delta V_c [(\lambda^2 - 1)/2] \quad (3)$$

The tangential strain may be computed by an iterative process based upon accumulation of small strains associated

Presented at the ARS Solid Propellant Rocket Conference, Philadelphia, Pa., January 30-February 1, 1963; revision received July 31, 1963.

* Chief, Propellant Physics Section, Chemistry Department, Member AIAA.

† Chemical Assistant, Propellant Physics Section, Chemistry Department, Member AIAA.

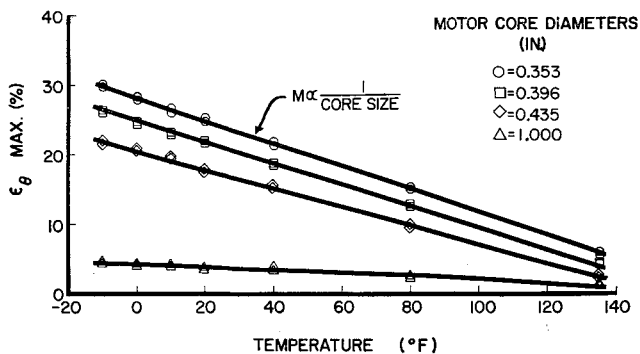


Fig. 1 Typical data from successive cool-down motors.

with successive slight changes in temperature. The limiting value of this iterative process is, of course, identical with the result obtained if natural (or logarithmic) strain is calculated from the total internal displacement imposed by a large change in temperature. Correlation of these strain values with the results of uniaxial tensile tests must, therefore, be made by using natural strains for the latter. It may be noted, incidentally, that for propellant grain configurations involving more complex geometries, such as star points, the strains may be increased because of stress concentrations.^{5, 6}

Temperature Conditioning of Model Test Motors

Test vehicles are employed in two basic types of experiments. The first experiment is designed to measure tangential strains from a given cavity diameter motor across a broad temperature range. After completion of cure, the motors are cooled slowly from the cure temperature in decrements of 10° or 20° to -80°F or until failure. The strains imposed by cooling are measured as described in the foregoing. Sufficient time is allowed at each temperature condition for complete temperature saturation,⁷ normally two days. Strain rates imposed by this experiment are of the order of $1 \times 10^{-4} \text{ min}^{-1}$. The decrements of cooling vary with the core size used in a particular experiment, since a small-cavity-diameter test motor will reach a high strain level at a relatively high temperature. Tangential strain data from various cavity diameter test motors are obtained during decremental cooling. Figure 1 demonstrates the effect of successive cooling on imposed strains within the model test vehicle.

The second type of experiment consists of temperature cycling conditioning. In this experiment, test motors are subjected to 24-hr conditioning at -10°F and are measured. Then they are immediately placed in conditioning for 24 hr at 135°F. This is defined as one cycle of temperature conditioning.

Model test motors were initially loaded with a very thin liner between the case and propellant grain. Recently, however, it has been shown that no difference in strain level is noted between motors loaded with normal liner materials, which rigidly bond the propellant grain to the case wall,

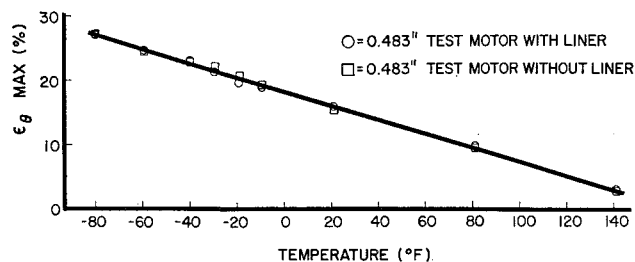


Fig. 2 Variation of maximum tangential strain with temperature for test motors with and without liner.

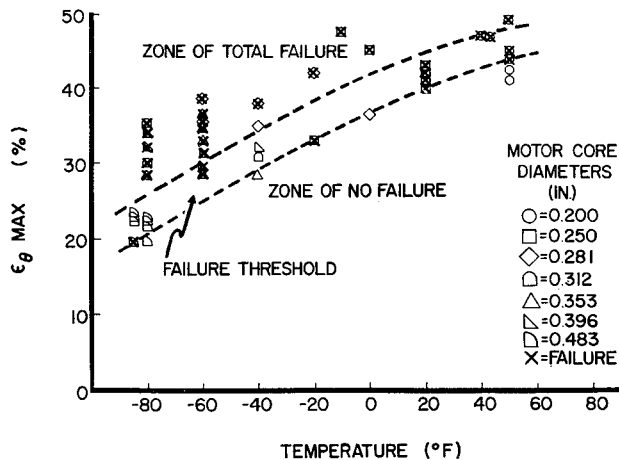


Fig. 3 Failure threshold of test motors.

and motors loaded without liner so that the propellant bonds directly to the motor case. In those instances where it is desired to reproduce prototype motor conditions closely, for example, effects of prolonged high-temperature aging prior to low-temperature conditions, liner is still used in the model motors so that its properties are tested along with those of the propellant. Figure 2 demonstrates the behavior of unlined and lined test motors.

The problem is to predict the temperature and strain at which a given motor will fail. When motors of various core diameters are subjected to decremental cool-down until grain failure is induced, the range of temperature and the tangential strains imposed when failure takes place at that temperature allow a failure threshold to be drawn, thus giving an indication of the limits of strain which a particular type of propellant will withstand in a given motor. Inasmuch as both laboratory failure data for propellants and strain associated with failure in the test vehicles must be represented by a distribution of values, any correlation between the two types of failure must be statistical in nature. Thus, the failure threshold, shown in Fig. 3, cannot be represented by a single line. Instead, it takes the form of a zone of failure with a range of approximately 7% strain between its boundaries.

One would desire next to correlate uniaxial tensile behavior with the failure threshold. Stress-strain curves of a typical propellant show a marked variation with temperature, as illustrated in Fig. 4. Figure 5 shows a superposition of the failure threshold curves on the uniaxial strain at the constant temperature under consideration and at a fixed nominal strain

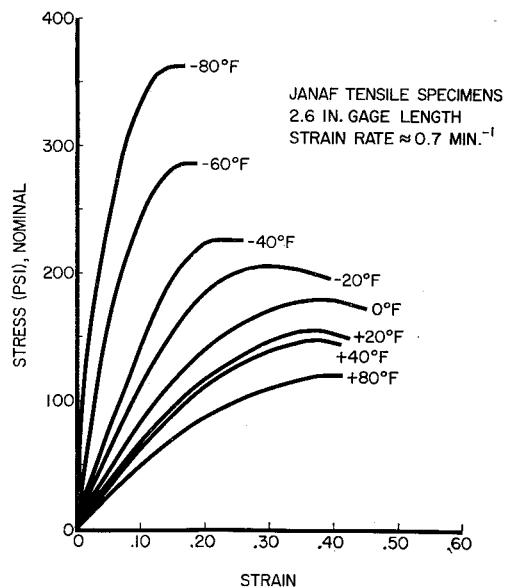


Fig. 4 Typical propellant stress-strain curves.

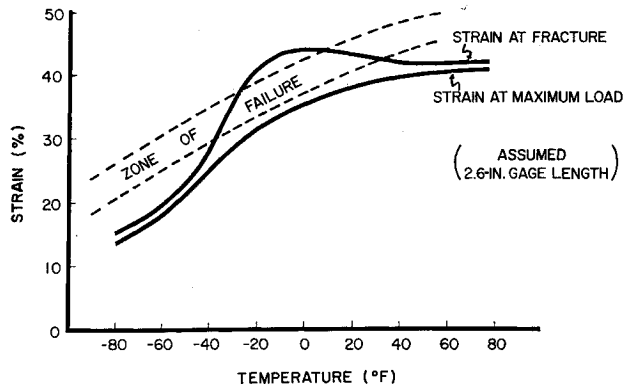


Fig. 5 Comparison of routine JANAF data with model failure.

rate of approximately 0.7 min^{-1} . The strain at fracture and the strain at maximum load curves shown in Fig. 5 are based upon average values of three tests at each of 12 temperatures. This method of comparison ignores any difference between the nominal strain rate (0.7 min^{-1}) and that thermal strain rate ($1 \times 10^{-4} \text{ min}^{-1}$) actually present. For this reason the foregoing technique is not an adequate general method of predicting motor failure limits, although, when relatively low failure strains are involved in short case-bonded charges with unrestrained ends, correlation of this type has been reported by Wiegand.⁸ This is attributed to a relative insensitivity of failure behavior to rate of loading under these conditions. Figure 6, however, shows that many of the motors studied at Thiokol have satisfactorily survived temperatures below the limit predicted in this way. Numerical comparison of failure in simple uniaxial tensile tests with failure of the same propellant in model test motors is shown in Table 1. As indicated previously, failure at various temperatures in the model test vehicles was obtained by varying the size of the internal perforation. This figure typifies a large number of results obtained from model test motors. The strains involved in many of these tests were low, because relatively large core sizes were used in order to approximate closely the strain requirements of the prototype motor that uses this propellant.

Another approach, which might be expected to represent a higher degree of approximation in predicting motor performance from laboratory measurements, uses the strain endurance capability. This is intended to eliminate time effects and to provide a minimum value for strain capability. It has been found, however, that strain endurance capability is a function of the rate at which the fixed strain was imposed on the specimen. Rate effects, therefore, are not eliminated by use of strain endurance capability as a criterion of motor performance. In the model test motors, rate of strain application is extremely low. Figure 7 represents the results of the effect of rate of strain application on endured strain. The results of this experiment show that lower rates of strain imposition result in lower strain endurance capabilities. It may be possible to correlate specialized strain endurance tests with motor performance, however,

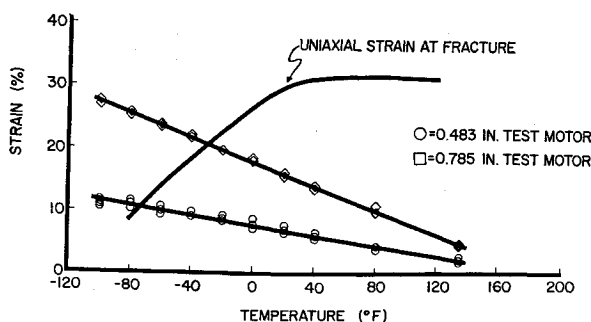


Fig. 6 Variation of strain with temperature.

Table 1 Typical propellant failure data

Temperature, °F	Uniaxial strain at maximum load, range	Uniaxial strain at fracture, range	Strain at failure in test vehicles, range
50			0.440-0.495
40	0.334-0.341	0.336-0.343	0.470-0.475
20	0.302-0.330	0.315-0.364	0.400-0.435
0	0.300-0.314	0.338-0.400	0.450
-10	0.298-0.335	0.388-0.393	0.475
-20	0.275-0.285	0.345-0.360	0.330-0.420
-40	0.205-0.210	0.300	0.375
-60	0.115-0.161	0.150-0.230	0.280-0.380
-80	0.110	0.143-0.150	0.280-0.350
-85			0.190

since the rate dependence of strain endurance is less at low rates of strain application, as indicated by Fig. 7. It appears that motor performance may be predicted by using uniaxial strain endurance data obtained at low rates ($\approx 1 \times 10^{-2} \text{ min}^{-1}$) of strain application.

Temperature cycling of model test motors is conducted to determine the temperature cycling capability of the propellant. The low temperature to which the test motor is cycled is selected on the basis of the strain level expected for a particular core size.

Another method of rapidly determining the low-temperature cycling limit, although it will not yield an absolutely accurate value for the limit, is to lower the low temperature to which the test motor is cycled 10°F every three cycles until the grain fails. As the number of cycles increases, the induced strains increase. In some cases, this may be due to the high-temperature (135°F) portion of the temperature cycle resulting in a post-cure effect with concomitant shrinkage of the propellant. It has been noted in repeated experiments that test motors of the same core size which have been temperature cycled and those which have been cooled to successively lower temperatures will fail at almost exactly the same level of strain. Figure 8 shows typical data supporting this correlation. From this correlation, it is possible to say that, at least in some cases, propellant grain failure is apparently dependent not on temperature but only on a certain level of strain. This may be explained by the fact that the rate of strain application in the test vehicle is extremely low. On a temperature-reduced rate basis, therefore, propellant response may be essentially the same over a considerable temperature range.

Experimental Technique

I. Apparatus

A. Refrigeration equipment

The equipment used for conditioning test motors includes mechanical refrigeration units capable of operation in the temperature range 40° to -80°F .

B. Intermediate temperature equipment

Conditioning equipment with both heating and cooling capability for operation in the temperature range from 100° to 40°F is used.

C. Ovens

High-temperature conditioning equipment operating in the temperature range from 100° to 170°F is used.

D. Radiographic equipment

X-ray profiles of the test motors are obtained in the 0° and 90° planes to determine the condition of the propellant grain and to measure displacements in the test motors.

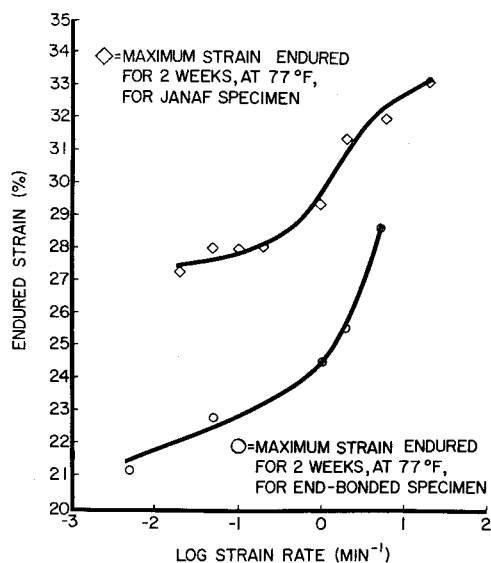


Fig. 7 Variation of strain endurance with rate of strain application.

II. Procedure

Two general types of conditioning are presently being employed:

A. Successive cool-down

A representative sample of test motors of any particular core size is decrementally cooled down to obtain the tangential strain at the environmental temperatures. A typical cool-down schedule would be cure temperature (on removal from cure), controlled ambient (77°), 40°, 20°, 0°, -20°, -40°, -60°, -80°, and -100°F. The schedule will vary with the core size used; smaller core diameter test motors will read a high strain at a relatively high temperature. Therefore, the low temperature would be deleted, and more high temperatures would be added. Two days at each temperature are allowed for complete temperature saturation of the propellant grain. Then the vehicle is x-rayed and immediately placed in the next lower step of conditioning. Two x rays are taken, one in the 0° plane, the other in the 90° plane. All motors are stored with 0° plane horizontal.

B. Temperature cycling

Representative tests motors of one or more core sizes are temperature-cycled between the limits of 135° and -10°F. One day at each temperature extreme is one full cycle. This procedure is usually conducted for five full cycles. However, the number of cycles may be varied. X rays are normally taken at $\frac{1}{2}$, $2\frac{1}{2}$, and $4\frac{1}{2}$ cycles of conditioning (cold side of cycle). Continued cycling until grain failure is induced gives an indication of the temperature cycling capability of a particular type of propellant.

C. Handling techniques

Regardless of the type of conditioning being conducted, certain precautionary measures are taken during the handling and measurement of the motors, especially at cold temperatures, to hold temperature change to the minimum and to prevent the accumulation of excess moisture on the propellant grains. These measures are as follows:

1) The number of motors removed from temperature conditioning at any given time is held to the minimum so that the propellant grains will be at the desired temperature at the time the actual x-ray profiles are made.

2) The ends of the motors are capped except when visual inspections are being made. This precaution essentially eliminates the accumulation of atmospheric moisture that

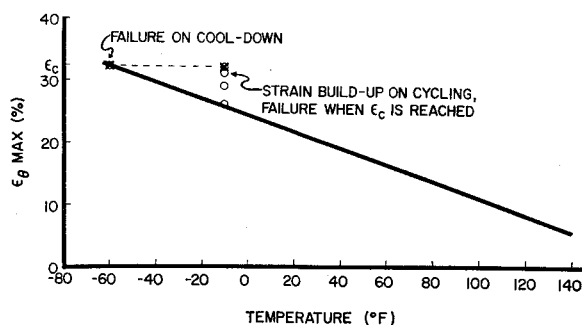


Fig. 8 Correlation of failure induced by temperature cycling with low-temperature failure.

tends to condense on the internal surface of the propellant when the grain is cold. In many cases, the cavities are purged with dry nitrogen gas prior to capping the ends to insure further the dryness of the grain. These measures are important in view of the known detrimental effects of excess moisture on propellants.

3) An insulated box is used to transport the motors to and from the x-ray facility. In this manner, temperature changes are held to the minimum.

III. Data Reduction

Core measurements are made at the axial center of the motor and at 1 in. on each side of center. The maximum diameter obtained in this region is then used to calculate tangential strain. Two methods are presently available to obtain this maximum cavity diameter.

A. Visual method

The x-ray film (0° plane) is placed over a "Portatrace" to illuminate the image on the film, and the measured core diameter at the center and at 1 in. on either side of the center is read to 1/10,000 in. by use of a vernier caliper. A magnification factor of 1.8% must be accounted for in calculation of actual core diameter. Tangential strain can be calculated by the following simple equation:

$$\epsilon_{\theta} = (D_1 - D_0C)/D_0C \quad (4)$$

where

- ϵ_{θ} = maximum tangential strain, decimal
- D_0 = original core diameter, in.
- D_1 = measured core diameter at test temperature, in.
- C = 1.018

B. Densitometer method

Use of a Jerrold Ash Densitometer is employed to determine more accurately the edge of the propellant cavity at any test temperature. As in the visual method, scans are made in the same motor position, and the corresponding

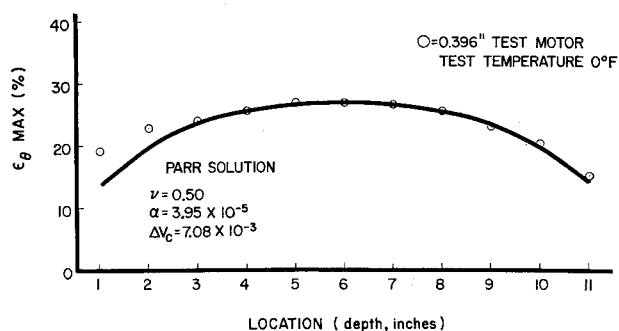


Fig. 9 Comparison of finite-difference solution with experimental data.

traces are reduced to obtain the actual core diameter at any test temperature. Equation (4) is employed to calculate maximum tangential strain.

Conclusions

Laboratory uniaxial tensile data, while valuable for comparative purposes in propellant development programs, generally do not provide the stress engineer with sufficient information upon which to base predictions of solid rocket motor performance. Rate effects, often neglected in testing for screening purposes, can introduce wide discrepancies between propellant strain capabilities as measured in constant-strain rate tests and the performance of propellant in a motor during low-temperature storage. Even strain endurance capability of propellant appears to be a time-dependent property, since it varies with the rate at which the constant strain was originally imposed on the propellant. Finally, test techniques have not been developed as yet to the point where adequate failure criteria for propellants in combined stress or strain states have been defined.

Model test motors are, therefore, of considerable usefulness in aiding the prediction of structural performance of solid rocket motors. A simple, cylindrical motor 2 in. in diameter and 12 in. long has been used successfully to define the threshold of propellant failure in terms of strain induced by low-temperature conditioning. Proper selection of the internal perforation in the test motor allows a comparison of strains experienced in the test motor with those experienced in prototype cylindrical core rocket motors. When the size of the internal perforations in such motors is small (≈ 0.25 in.), strain relief due to "end effects" is apparent over the entire length of the motor. A finite difference

solution is appropriate in such cases.² An example of the results that can be obtained by this technique is shown in Fig. 9. To achieve a plane strain condition, the length of the motor should be increased. When larger internal perforations are employed, a finite-length section of uniform maximum strain is observed at the axial center of the motor, suggesting that the propellant in this region approaches a state of plane strain.

References

- Wiegand, J. H., "Study of mechanical properties of solid rocket propellants," Aerojet-General Corp. Rept. 0411-10F (March 1962).
- Ignatowski, A. J. and Jenkins, L. W., "Polymer physics," Rohm & Haas Co., Progr. Rept. on Interior Ballistics, P-62-1 (August 1962).
- Parr, C. H., "End effects due to shrinkage in solid propellant grains," Bull. Twentieth Meeting, JANAF-ARPA-NASA Panel on Physical Properties, Vol. I, SPIA/PP14U, p. 71 (October 1961).
- Williams, M. L., Blatz, P. J., and Shapery, R. A., "Fundamental studies relating to systems analysis of solid propellants," Graduate Aeronaut. Lab., Calif. Inst. Tech. SM61-5 (February 1961).
- Fourney, M. E. and Parmerter, R. R., "Stress-concentration data for internally perforated star grains," Naval Ordnance Test Station TP 2728, Bur. Naval Weapons 7758 (December 1961).
- Williams, M. L., "Some thermal stress design data for rocket grains," ARS J. 29, 260-267 (1959).
- Medford, J. E., "Measurement of thermal diffusivity of solid propellants," ARS J. 32, 1390-1392 (1962).
- Wiegand, J. H., "Recent advances in mechanical properties evaluation of solid propellants," ARS J. 32, 521-527 (1962).

OCTOBER 1963

AIAA JOURNAL

VOL. 1, NO. 10

Nonuniform Shrinkage of a Hollow Viscoelastic Cylinder

A. S. ÇAKMAK*

Princeton University, Princeton, N. J.

The effects of nonuniform shrinkage on stresses and displacements of a thick-walled, hollow cylinder of viscoelastic material are discussed, for the case of plane strain, as a function of the loading rate. The cylinder is contained in a rigid casing resulting in zero circumferential and radial displacements at the outer surface. The inner surface is free of tractions. The problem is solved using the elastic-viscoelastic analogy, where the deviatoric behavior is characterized by the standard solid, and the volumetric behavior is taken to be elastic. The results indicate a strong dependence of radial displacements and principal stresses on the loading rate. The maximum values of the principal stresses show a marked reduction and smaller deviations from their final values for decreasing values of the loading rate. The radial displacements exhibit little change in deviation from their final values for changes of the loading rate.

Nomenclature

λ, μ	= Lamé's constants
r, z	= cylindrical coordinates
u_r	= radial displacement
σ_r	= radial stress component
σ_θ	= circumferential stress component
ϵ_r	= radial strain component
ϵ_θ	= circumferential strain component
S_{ij}	= deviatoric stress components
e_{ij}	= deviatoric strain components
θ	= rate of loading parameter

E	= Young's modulus
γ	= Poisson's ratio
G	= shear modulus
K	= bulk modulus
μ_m	= viscosity
δ_{ij}	= Kronecker delta
\mathbf{G}	= viscoelastic shear modulus
\mathbf{K}	= viscoelastic bulk modulus
T	= temperature
δT	= difference in temperature
τ	= relaxation time
$H(t)$	= Heaviside step function
C_1, C_2	= integration constants
a	= inner radius
b	= outer radius
L	= Laplace transform
L^{-1}	= inverse Laplace transform
S	= Laplace transform parameter

Received March 4, 1963; revision received July 24, 1963. This research was supported by the Office of Naval Research under Contract Nonr 266(78) during the author's residence at Columbia University.

* Assistant Professor of Civil Engineering, Department of Civil Engineering, School of Engineering and Applied Science.